

Kinetic modelling of shielding and amplification of RMPs by the tokamak plasma*

M. F. Heyn¹, I. B. Ivanov^{1,3}, S. V. Kasilov^{1,2}, W. Kernbichler¹, P. Leitner¹ V. Nemov^{1,2}

¹*Association EURATOM-ÖAW, Inst. for Theor. and Comput. Physics, TU Graz, Austria*

²*Inst. of Plasma Physics, NSC “Kharkov Institute of Physics and Technology”, Ukraine*

³*Petersburg Nuclear Physics Institute, Russia*

Introduction

ELM mitigation by resonant magnetic field perturbations (RMPs) is presently a subject of intensive experimental and theoretical studies. As shown in Ref. [1] and other references, RMPs are strongly shielded by plasma currents if the perpendicular electron fluid velocity $V_{\perp e}$ is finite. As a result, plasma shielding prevents the formation of ergodic layers which were originally thought to be responsible for ELM mitigation. Recently in Ref. [2] it has been found that in one of the successful ELM mitigation experiments on DIII-D, the point $V_{\perp e} = 0$ where the field is not shielded, is located at the top of the pedestal. Based on this finding, in Ref. [3] significant quasilinear effects of RMPs on the pedestal plasma have been demonstrated. On the other hand, in this discharge, not only a $V_{\perp e} = 0$ point but also a reversal point of the radial electric field $E_r = 0$ is present in the pedestal region as shown in Fig. 1 of Ref. [2]. The substantial effect of $E_r = 0$ points on RMP penetration and RMP driven plasma transport is studied in the present contribution.

Kinetic plasma response model

The linear plasma response model is based on the cylindrical tokamak model where toroidicity effects are ignored. Maxwell equations

$$\nabla \times \tilde{\mathbf{E}} = \frac{i\omega}{c} \tilde{\mathbf{B}}, \quad \nabla \times \tilde{\mathbf{B}} = -\frac{i\omega}{c} \tilde{\mathbf{E}} + \frac{4\pi}{c} \tilde{\mathbf{j}}, \quad (1)$$

are solved using the current density obtained from the solution of the linearised kinetic equation in terms of a Green's function,

$$i [k_{\parallel} v_{\parallel} + k_{\perp} v_{E\perp} - m_{\phi} \omega_c - \omega] G_{\mathbf{m}}(v_{\parallel}, v'_{\parallel}) - \hat{L}_{cp} G_{\mathbf{m}}(v_{\parallel}, v'_{\parallel}) = \delta(v_{\parallel} - v'_{\parallel}). \quad (2)$$

Here, \hat{L}_{cp} is an Ornstein-Uhlenbeck type collision operator,

$$\hat{L}_{cp} f_1 = \hat{L}_c f_1 + \hat{L}_{cI} f_1, \quad \hat{L}_c f_1(v_{\perp}, v_{\parallel}) = v v_T^2 \frac{\partial}{\partial v_{\parallel}} \left(\frac{\partial}{\partial v_{\parallel}} + \frac{v_{\parallel}}{v_T^2} \right) f_1(v_{\perp}, v_{\parallel}) \quad (3)$$

with an additional term to make the collision operator energy conserving

$$\hat{L}_{cI} f_1(v_{\perp}, v_{\parallel}) = \frac{v}{\sqrt{2\pi v_T}} \exp\left(-\frac{v_{\parallel}^2}{2v_T^2}\right) \left(\frac{v_{\parallel}^2}{v_T^2} - 1\right) \int_{-\infty}^{\infty} dv'_{\parallel} \left(\frac{v'^2_{\parallel}}{v_T^2} - 1\right) f_1(v_{\perp}, v'_{\parallel}). \quad (4)$$

*This work, supported in part by the European Commission under the contract of Associations between EURATOM and the Austrian Academy of Sciences, was carried out within the framework of the European Fusion Development Agreement. The views and opinions expressed herein do not necessarily reflect those of the European Commission.

Subscript $\mathbf{m} = (m_\phi, m_\vartheta, k_z)$ denotes Fourier harmonics over gyrophase, poloidal wavenumber and wavevector along the cylinder axis. The linear plasma current density is determined by moments of the perturbed distribution function

$$f_{\mathbf{m}} = -e \int_{-\infty}^{\infty} dv'_{\parallel} G_{\mathbf{m}}(v_{\parallel}, v'_{\parallel}) \left[\left(\tilde{\mathbf{E}} + \frac{1}{c} \mathbf{v} \times \tilde{\mathbf{B}} \right) \cdot \frac{\partial f_0}{\partial \mathbf{p}} \right]_{\mathbf{m}}, \quad (5)$$

where $(\tilde{\mathbf{E}}, \tilde{\mathbf{B}})$ is the perturbation field and f_0 is a shifted Maxwellian. A finite Larmor radius expansion of this function in Refs. [4, 1, 5] gives for the plasma current density

$$\tilde{j}_{(N)}^k(r, \vartheta, z) = \frac{1}{r} \sum_{n, n'=0}^N (-1)^n \frac{\partial^n}{\partial r^n} \left(r \sigma_{(n, n')}^{kl}(r, \mathbf{k}) \frac{\partial^{n'}}{\partial r^{n'}} \tilde{E}_l(r, \vartheta, z) \right). \quad (6)$$

In the first order expansion $N = 1$ and a static perturbation field $\omega = 0$, the gyroaveraged perturbed distribution function corresponding to $m_\phi = 0$ can also be obtained from the gyrokinetic equation. This function determines quasilinear particle and energy fluxes given respectively by

$$\Gamma = \frac{1}{2} \text{Re} \sum_{\mathbf{m}} \int d^3 p a_1 f_{\mathbf{m}} v_{\mathbf{m}}^{r*} = -n(D_{11}A_1 + D_{12}A_2), \quad (7)$$

$$Q = \frac{1}{2} \text{Re} \sum_{\mathbf{m}} \int d^3 p a_2 f_{\mathbf{m}} v_{\mathbf{m}}^{r*} = -nT(D_{21}A_1 + D_{22}A_2). \quad (8)$$

Here, $a_1 = 1$, $a_2 = m(v_{\perp}^2 + v_{\parallel}^2)/(2T)$, and the thermodynamic forces A_1, A_2 are related to gradients of the equilibrium plasma parameters as

$$A_1 = \frac{1}{n} \frac{\partial n}{\partial r} - \frac{e}{T} E_r - \frac{3}{2T} \frac{\partial T}{\partial r}, \quad A_2 = \frac{1}{T} \frac{\partial T}{\partial r}. \quad (9)$$

Diffusion coefficients D_{kl} are expressed through the perturbed radial guiding center velocity $v_{\mathbf{m}}^r$

$$D_{kl} = \frac{\pi m^3}{n} \text{Re} \sum_{\mathbf{m}} \int_0^{\infty} dv_{\perp} v_{\perp} \int_{-\infty}^{\infty} dv_{\parallel} \int_{-\infty}^{\infty} dv'_{\parallel} G_{\mathbf{m}}(v_{\parallel}, v'_{\parallel}) \times v_{\mathbf{m}}^{r*}(v_{\perp}, v_{\parallel}) v_{\mathbf{m}}^r(v_{\perp}, v'_{\parallel}) a_k(v_{\perp}, v_{\parallel}) a_l(v_{\perp}, v'_{\parallel}) f_0(v_{\perp}, v'_{\parallel}). \quad (10)$$

$$v_{\mathbf{m}}^r = \frac{v_{\parallel}}{B_0} B_{\mathbf{m}}^r - \frac{ick_{\perp}}{B_0} \Phi_{\mathbf{m}} - \frac{ik_{\perp} v_{\perp}^2}{2\omega_{c0} B_0} B_{\mathbf{m}\parallel} - \frac{ik_{\parallel} v_{\parallel}^2}{\omega_{c0} B_0} B_{\mathbf{m}\perp}, \quad (11)$$

Another important quantity, the toroidal torque density onto the particular species, is obtained from the force-flux relation

$$T_{\phi} = -\frac{e}{c} \sqrt{g} B_0^{\vartheta} \Gamma, \quad (12)$$

where \sqrt{g} and B_0^{ϑ} are the unperturbed metric determinant and the contra-variant poloidal magnetic field component. The first two terms in (11) describe parallel streaming and $\mathbf{E} \times \mathbf{B}$ drift and are much larger than the other two terms which describe magnetic drifts in the regions around the resonant surface. The former terms produce particle and energy fluxes due to the mismatch of the perturbed magnetic surfaces and the perturbed equipotential surfaces. This mismatch is absent in an ideal plasma where the latter two terms in (11) become important since they produce the neoclassical toroidal viscous torque. Due to energy conservation in the collision operator, the diffusion matrix is Onsager-symmetric. Without this property, the first two terms in (11) would lead to a non-zero (fake) energy flux even in the case of an ideal plasma and neglecting magnetic drifts, i.e., the last two terms in (11).

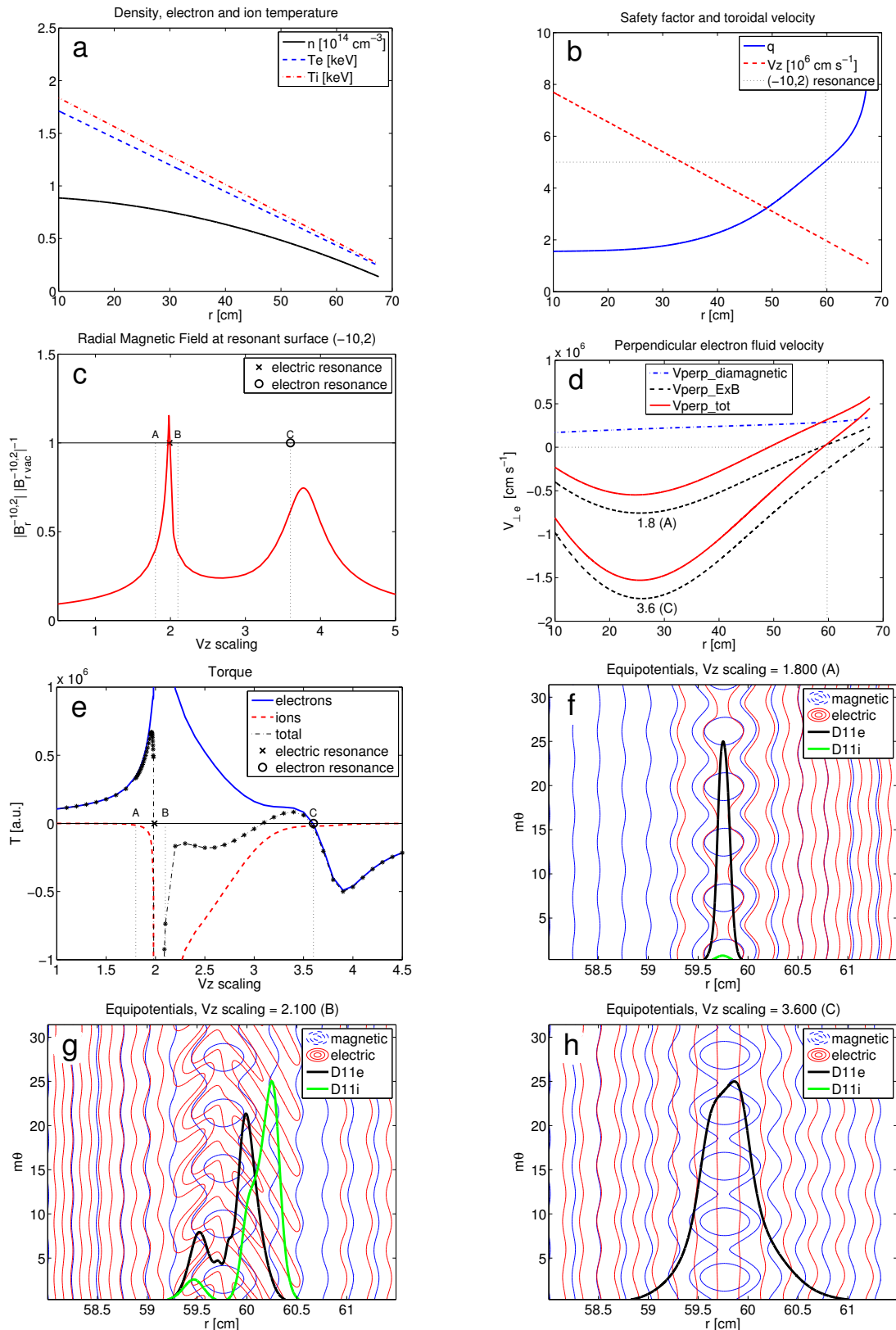


Fig. 1. a) Linear temperature and quadratic density profiles. b) Safety factor and linear toroidal velocity profile. c) V_z scaling dependence of $B_r(r_{\text{res}})$. d) Perpendicular electron fluid velocities for two different V_z scalings. e) Torque acting on electrons (blue), on ions (red) and total torque (black). f-h) Magnetic surfaces, equipotential surfaces, electron (black) and ion (green) D_{11} diffusion coefficients for the 3 different V_z scalings (A), (B) and (C) shown in c).

Results and discussion

In the present context, the model is applied to a low temperature discharge in a mid-size tokamak with linear temperature and parabolic density profiles shown in Fig. 1a and linear profile of the toroidal rotation velocity V_z shown in Fig. 1b. Together with the pressure gradients, the toroidal velocity determines the radial electric field. For modelling purposes this field is modified by scaling the toroidal velocity V_z .

The chosen perturbation mode ($m=-10$, $n=2$) is resonant at the plasma edge (see Fig. 1b). Scaling V_z places either the zero of total perpendicular electron fluid velocity $V_{\perp e} = 0$ (scaling factor 3.6) or the zero of the radial electric field, $E_r = 0$ (scaling factor 1.8) to the resonant surface as shown in Fig. 1d. In both cases, plasma shielding of the perturbation is highly reduced and the radial component \tilde{B}_r at the resonant surface increases almost to its vacuum value. This increase is more significant when the $E_r = 0$ point crosses the resonance (see Fig. 1c).

The behaviour of ion and electron torques computed as volume integrals of the torque densities (12) is quite different around those resonances. This can be seen in Fig. 1e. The electron torque, normally much larger than the ion torque, shows a typical reversal behavior at the electron fluid velocity zero. This increased torque is a consequence of the increased perturbation field in a plasma with density and temperature gradients. In this case, the total torque is basically the electron torque and particle fluxes are non-ambipolar. The increase in particle transport is accompanied by a change in the plasma toroidal rotation.

Near the $E_r = 0$ point both torques increase strongly in amplitude but balance each other and the total torque stays small. Thus, the increased particle transport is almost ambipolar and the toroidal rotation changes little. The origin for the increased ambipolar transport near $E_r = 0$ is seen from looking at the perturbed magnetic surfaces (blue) and perturbed equipotential surfaces (red) which are shown together with the electron (blue) and ion (green) diffusion coefficients D_{11} in Figs. 1f-1h. The unperturbed potential has an extremum at $E_r = 0$ and equipotentials are much more perturbed around this resonance than anywhere else.

Convective cells are formed due to the ambipolar $\mathbf{E} \times \mathbf{B}$ drift of the plasma along those equipotentials. This leads to a strong increase of the ambipolar particle transport. The increased transport might be responsible for the density pump-out usually observed in ELM mitigation experiments. The $E_r = 0$ resonance region is fairly slim and, therefore, the parameter window where it can affect the pedestal is rather narrow.

References

- [1] M. F. Heyn, I. B. Ivanov, S. V. Kasilov, W. Kernbichler, J. Ilon, R. A. Moyer, and A. M. Runov, *Nucl. Fusion* **48**, 024005 (2008).
- [2] I. Joseph, *Contrib. Plasma Phys.* **52**, 326 (2012).
- [3] F. L. Waelbroeck, I. Joseph, E. Nardon, M. Bécoulet, and R. Fitzpatrick, *Nucl. Fusion* **52**, 074004 (2012).
- [4] M. F. Heyn, I. B. Ivanov, S. V. Kasilov, and W. Kernbichler, *Nuclear Fusion* **46**, S159 (2006).
- [5] I. B. Ivanov, S. V. Heyn, M. F. and Kasilov, and W. Kernbichler, *Physics of Plasmas* **18**, 022501 (2011).